

Capabilities of long-baseline experiments in the presence of a sterile neutrino

Debajyoti Dutta,^{1,*} Raj Gandhi,^{1,†} Boris Kayser,^{2,‡}

Mehedi Masud,^{1,§} and Suprabh Prakash^{e1,3,**}

¹*Harish-Chandra Research Institute,*

Chhatnag Road, Jhansi, Allahabad 211019, India

²*Theoretical Physics Department, Fermilab,*

P.O. Box 500, Batavia, IL 60510 USA

³*School of Physics, Sun Yat-Sen (Zhongshan) University,*

Guangzhou 510275, P. R. China

(Dated: July 8, 2016)

^e Corresponding author

Abstract

Assuming that there is a sterile neutrino, we ask what then is the ability of long-baseline experiments to i) establish that neutrino oscillation violates CP, ii) determine the three-neutrino mass ordering, and iii) determine which CP-violating phase or phases are the cause of any CP violation that may be observed. We find that the ability to establish CP violation and to determine the mass ordering could be very substantial. However, the effects of the sterile neutrino could be quite large, and it might prove very difficult to determine which phase is responsible for an observed CP violation. We explain why a sterile neutrino changes the long-baseline sensitivities to CP violation and to the mass ordering in the ways that it does. We note that long-baseline experiments can probe the presence of sterile neutrinos in a way that is different from, and complementary to, the probes of short-baseline experiments. We explore the question of how large sterile-active mixing angles need to be before long-baseline experiments can detect their effects, or how small they need to be before the interpretation of these experiments can safely disregard the possible existence of sterile neutrinos.

PACS numbers: 14.60.St,14.60.Pq,14.60.Lm,13.15.+g

Keywords: Leptonic CP Violation, Sterile neutrinos, Long-Baseline experiments, DUNE, NO ν A, T2K, T2HK

* Email Address: debajyotidutta@hri.res.in

† Email Address: raj@hri.res.in

‡ Email Address: boris@fnal.gov

§ Email Address: masud@hri.res.in

** Email Address: prakash3@mail.sysu.edu.cn

I. INTRODUCTION

Much of the activity in neutrino oscillation experiments over the past two decades has focused on the increasingly precise determination of a) the neutrino mass-squared differences, $\delta m_{ij}^2 = m_i^2 - m_j^2$, and b) the mixing angles θ_{ij} along with the attendant CP phase δ_{CP} , which constitute the PMNS [1–3] mixing matrix $U_{\alpha i}$, with $i, j = 1, 2, 3$ & $i \neq j$ and $\alpha = e, \mu, \tau$. The complex matrix U parameterizes the overlap between the neutrino mass eigenstates ν_i and the flavour eigenstates ν_α . While considerable progress has been achieved towards determining the mixing angles and mass differences to appreciable accuracy, the CP phase δ_{CP} remains almost completely unknown.

The sources and qualitative nature of the experiments that have helped in this determination have been diverse, with neutrinos from the atmosphere, from reactors, from the sun and from particle accelerators being observed at detectors placed at baseline lengths spanning a wide range and employing a variety of detection techniques [4–16]. Global analyses [17–19] of the data collected have aided the consolidation of these efforts. This, in turn, has led to the gradual build-up of a consistent three family neutrino paradigm in impressive conformity with what is known, both theoretically and experimentally, about the lepton and quark sectors of the highly successful Standard Model (SM) of particle physics (when extended, nominally, to include massive neutrinos). Additionally, these experimental and theoretical efforts have helped formulate immediate questions that need to be answered by ongoing and planned experiments, which include the determination of a) the presence or absence of CP violation (CPV) in the lepton sector, and b) the mass hierarchy (MH), or ordering, of the neutrino mass eigenstates.

Nonetheless, there are several ripples in this seemingly smooth fabric, at least some of which could be indicative of underlying new physics (for a discussion see [20]). Such physics, if real, could affect the interpretation and sensitivities of present and planned experiments. One such issue relates to signals from a variety of short-baseline experiments [21–25], which hint at the possible existence of short-wavelength oscillations, driven by one or more largely sterile states (*i.e.* states that do not have standard weak interactions, but couple indirectly via mixing) with $O(1 \text{ eV}^2)$ mass-squared splittings that are significantly larger than the two splittings that characterize the standard 3 family paradigm (referred to in what follows as the 3+0 scenario). These short-wavelength oscillations can have significant effects when the

(Baseline L)/(Energy E) of neutrinos in a beam is ~ 1 km/GeV.

It is generally true, of course, that for significantly larger values of L/E , the short-wavelength oscillations driven by the large splittings involving an extra neutrino ν_4 will be averaged to an L/E -independent value by the finite energy resolution of a typical detector. However, even the presence of a single additional sterile neutrino mass eigenstate (referred to as the 3+1 scenario in what follows) introduces three additional mixing angles and two additional phases capable of significantly affecting oscillations at large baselines [26, 27]. It has been shown in [27], using the 1300 km Deep Underground Neutrino Experiment (DUNE) as an example, that if such a neutrino exists in nature, long-baseline results, interpreted without taking the short-wavelength oscillations into account, could erroneously imply that CP violation is very small or totally absent, when in reality it could be very large. In addition, measurements interpreted as determining the CP-violating phase in the standard 3+0 paradigm could in fact be measuring a linear combination of one or more phases belonging to the 3+1 sector. These effects, which arise from large interference terms (between the 3+0 and 3+1 sectors) in the appearance probability, are accentuated by the presence of matter, which brings in contributions from sterile-sector mixings and phases that are quiescent at short baselines. Thus, the presence of the 3+1 (or, more generally, $3 + n$) sector can significantly blur any conclusions regarding CPV that may be drawn by long-baseline experiments.

Suppose that a ~ 1 eV mass largely-sterile neutrino does exist. What then is the ability of long-baseline experiments to establish that the leptonic weak interactions violate CP, to determine the mass-ordering of the three established neutrinos, and to determine which CP-violating phase or phases is responsible for any CP violation that may be observed? In this paper, we address these questions. We find that the capacity to establish CP violation and to determine the mass ordering could be very substantial. However, the effects of the extra neutrino could be quite large, and could lead to erroneous or ambiguous conclusions, as already found in the earlier work [27]. We display examples that demonstrate the difficulty involved in determining which phase is causing an observed CP violation.

This work thus carries forward the approach adopted in [27]. Specifically, we study how expected sensitivities to the MH and CPV at NOvA [28], T2K [10], DUNE [29, 30] and HyperKamiokande (HK) [31] are altered in the 3+1 scenario. Some of the other questions we attempt to answer are focused on DUNE as an example. For instance, suppose that

the planned program of short-baseline experiments [32–35] that will probe the existence of 1eV-mass sterile neutrinos does not see anything. We ask how tightly one must then bound the sterile-active mixing angles to ensure that DUNE data can be safely interpreted without taking the possible existence of sterile neutrinos into account.

Early work examining the effects of sterile neutrinos at long baselines includes several studies of neutrino factories at baselines of 3000 km - 7500 km, with muon energies in the range 20 GeV - 50 GeV, focusing on effects at both near and far detectors [36–40]. More recent work [26] includes a study of effects relevant to T2K [10] and a combined study [41] for T2K, MINOS [42] and reactor experiments. Additionally, issues having some overlap with those addressed here for DUNE have been discussed in [43]. Recently, in [44] the effects of one additional mass eigenstate at long baselines have been studied, and sensitivity calculations in the presence of a sterile state have been presented in [45, 46].

In Section II below we define our mixing matrix parametrisation, describe our numerical simulation procedure and specify the constraints that motivate the parameter ranges we use in the simulation. We also provide brief descriptions and salient specifications for the long-baseline experiments considered in our work. Section III gives the results on mass hierarchy and CP sensitivities in the presence of a sterile neutrino and discusses the reasons why they differ substantially from the 3+0 case. This section also addresses the question of how large sterile-active mixing angles need to be before measurable effects show up at long-baselines, and how small they need to be such that their presence can be safely ignored when interpreting the results of experiments. Section IV provides the conclusions and summarizes the results of the paper.

II. INPUTS AND CALCULATIONAL PROCEDURES FOR THE 3+1 SCENARIO

A. The 3+1 mixing matrix

We begin by specifying our parameterisation for the PMNS matrix in the presence of a sterile neutrino;

$$U_{\text{PMNS}}^{3+1} = O(\theta_{34}, \delta_{34})O(\theta_{24}, \delta_{24})O(\theta_{14})O(\theta_{23})O(\theta_{13}, \delta_{13})O(\theta_{12}) \quad (1)$$

Here, in general, $O(\theta_{ij}, \delta_{ij})$ is a rotation matrix in the ij sector with associated phase δ_{ij} . For example,

$$O(\theta_{24}, \delta_{24}) = \begin{pmatrix} 1 & 0 & 0 & 0 \\ 0 & \cos \theta_{24} & 0 & e^{-i\delta_{24}} \sin \theta_{24} \\ 0 & 0 & 1 & 0 \\ 0 & -e^{i\delta_{24}} \sin \theta_{24} & 0 & \cos \theta_{24} \end{pmatrix}; O(\theta_{14}) = \begin{pmatrix} \cos \theta_{14} & 0 & 0 & \sin \theta_{14} \\ 0 & 1 & 0 & 0 \\ 0 & 0 & 1 & 0 \\ -\sin \theta_{14} & 0 & 0 & \cos \theta_{14} \end{pmatrix} \text{ etc.}$$

In this parametrization, although the the vacuum $\nu_\mu \rightarrow \nu_e$ oscillation probability is independent of the 3-4 mixing angle and the associated CP phase, the presence of matter brings about a dependence on all mixing angles and phases. Specifically, unlike the vacuum case, the 3-4 mixing angle and its associated phase are no longer dormant, and the 3+1 electron neutrino appearance probability at long baselines exhibits a significant dependence on them. Additionally, there are interference terms that enter for non-zero values of the phases that are not necessarily small, especially in the presence of matter, *e.g.*, the term proportional to the sine of the sum of the phases δ_{13} and δ_{24} [27, 47].

B. Simulation Procedure

In this section, we describe the details of the simulation technique adopted in estimating the sensitivities and other results obtained. We have used the GLoBES [48, 49] software package for performing all our analyses. For extending the simulation to the 3+1 scenario, we used [50, 51]; which is an add-on to the default GLoBES software. Our assumptions regarding the values and ranges of the oscillation parameters for the 3+0 sector are as follows.

- θ_{12} and θ_{13} are taken to be 33.48° and 8.5° respectively [52].
- δm_{21}^2 is taken to be $7.5 \times 10^{-5} \text{ eV}^2$ while δm_{31}^2 is set to be $2.457 \times 10^{-3} \text{ eV}^2$ ($-2.374 \times 10^{-3} \text{ eV}^2$) for NH (IH) [52].
- The currently-allowed 3σ range on θ_{23} is $[38.3^\circ, 53.3^\circ]$ with the best fit at $42.3^\circ(49.5^\circ)$ for NH (IH) [52]. The θ_{23} best fit values from the global analyses [19, 53] are somewhat different from [52]. In this work, we make the simplifying assumption that 2-3 mixing is maximal; i.e. $\theta_{23} = 45^\circ$. However, the conclusions we draw also apply to non-maximal 2-3 mixing.

It is anticipated that even if the 3+0 scenario is not realised in nature, the above values and ranges will still hold to a very good approximation.¹

We draw information regarding the value of δm_{41}^2 from [55], which does a combined analysis of the global data. The best fit of δm_{41}^2 in the 3+1 scheme is found to be 0.93 eV^2 (Table 8 of [55]). In our work, we assume δm_{41}^2 to be $+1 \text{ eV}^2$ ² along with

$$\delta m_{41}^2 \sim \delta m_{42}^2 \sim \delta m_{43}^2 \gg |\delta m_{31}^2| \sim |\delta m_{32}^2| \gg \delta m_{21}^2 \quad (2)$$

Our assumed ranges for the sterile sector mixing angles corresponding to the 3+1 scenario draw upon current constraints and are as follows. Note that we derive the constraints correlated with the new mass-squared difference; i.e., the values of mixing angles that are compatible with $\delta m_{41}^2 \sim 1 \text{ eV}^2$ are chosen.

- Measurements at the Daya Bay experiments put constraints on the effective mixing angle in the electron anti-neutrino disappearance channel. This effective mixing angle is the same as θ_{14} under the choice of PMNS parameterisation in this work. Based on [56], we assume $\theta_{14} \leq 13^\circ$ at 95% C.L. Slightly tighter constraints are available from the BUGEY experiment; but at 90% C.L. [57]
- The strongest constraints on the 2-4 mixing angle can be derived from the IceCube data [58]. With their current data, only $\theta_{24} \leq 7^\circ$ can be allowed at 99% C.L.
- The MINOS experiment with its observed charged-current and neutral-current events spectra can constrain the 3-4 mixing angle. From [59], we have $\theta_{34} \leq 26^\circ$ at 90% C.L.

We also vary δ_{13} , δ_{24} and δ_{34} for 3+1 and δ_{CP} for 3+0 over the full possible range of $[-180^\circ, 180^\circ]$. Finally, the fluxes we use are identical to those used in [60]³. Details regarding the calculation of Poissonian χ^2 , treatment of systematic uncertainties etc. can be found in [48, 49].

¹ Some of our early calculations showed that the disappearance data *at the far detector* are less affected by the active-sterile mixing angles compared to the appearance data. Thus, the measurements that depend on $P_{\mu\mu}$, like $\sin^2 2\theta_{23}$ or $|\delta m_{31}^2|$, are expected to change less with the change of theoretical framework from 3+0 to 3+1. Likewise, it was shown in [54] that θ_{13} measurements at the reactor neutrino experiments will be robust even if there are sterile neutrinos. Also see [44] regarding this.

² The choice $\delta m_{41}^2 \sim 1 \text{ eV}^2$ is made because it is a convenient benchmark. We have checked that our results and conclusions remain qualitatively valid for the mass splitting range $0.1 - 10 \text{ eV}^2$. Numerical differences in an important calculated quantity like the event rate, for instance, between our benchmark choice and the upper and lower bounds of this range are of the order of 10%, and will bring about corresponding changes in calculations of sensitivities and other quantities calculated in our paper.

³ These differ slightly in intensity and peak value from the present version used by the DUNE collaboration, but these differences do not affect our conclusions in any substantive manner.

C. Details of Experiments

T2K and T2HK

The Tokai to Kamioka (T2K) experiment is an ongoing neutrino experiment in Japan whose main goals are to observe $\nu_\mu \rightarrow \nu_e$ oscillations and to measure θ_{13} . It may, however, be in a position to provide hints on CPV and the hierarchy, especially when its data are used in conjunction with those of other experiments. Neutrino beams generated at the J-PARC accelerator facility in Tokai are directed towards a 22.5 kton water Čerenkov detector placed in Kamioka, 295 km away at a 2.5° off-axis angle [61]. The ν_μ beam peaks sharply at 0.6 GeV, which is very close to the first oscillation maximum of the $\nu_\mu \rightarrow \nu_e$ appearance probability, $P_{\mu e}$. The flux falls off quite rapidly, such that it is negligible at energies greater than 1 GeV. The beam power is 750 kW, with a proton energy of 30 GeV, for runs in both the ν and $\bar{\nu}$ modes. Combining both runs, the experiment will gather a total exposure of $\sim 8 \times 10^{21}$ protons on target (POT). The neutrino flux is monitored by the near detectors, located 280 m away from the point of neutrino production. Details regarding the detector efficiencies and background events used in our work have been taken from [48].

The T2HK experiment [31], in essence, is a scaled-up version of the T2K experiment. It will accumulate 1.56×10^{22} protons on target with a 30 GeV proton beam. The detector size is expected to be 25 times the T2K detector. For both T2K and T2HK, we have assumed 2.5% (5%) signal and 20% (5%) background normalisation errors in ν_μ (ν_e) signal. All details regarding signal and background events and detector efficiencies for T2HK are taken from [31, 62].

NO ν A

The NuMI⁴ Off-axis ν_e Appearance experiment (NO ν A) [28] is an ongoing long-baseline super-beam experiment in the US. It aims to determine the mass hierarchy, θ_{13} , the octant of θ_{23} , and perhaps leptonic CP-violation, by the measurement of $\nu_\mu \rightarrow \nu_e$ oscillations. The source of ν_μ is the Fermilab's NuMI beamline. A 14 kton Totally Active Scintillator Detector (TASD) is placed in Ash River, Minnesota, which is 810 km away at an off-axis angle of 14 mrad (0.8°). This off-axis narrow-width beam peaks at 2 GeV. The experiment is scheduled to run for 3 years in ν mode and 3 years in $\bar{\nu}$ mode with a NuMI beam power of 0.7 MW and 120 GeV proton energy, corresponding to 6×10^{20} POT per year. A 0.3 kton near detector

⁴ Neutrinos at the Main Injector

is located at the Fermilab site. We assume 5% (2.5%) signal normalisation error for ν_e (ν_μ) signal. Assumed background error is 10%. The details of signal and background events and the detector efficiencies have been taken from [63].

DUNE

DUNE, a future experiment scheduled to come online ~ 2025 , (with specifications very similar to LBNE [29, 30]), will be located in the United States. It is a super-beam experiment with the main aim of establishing or refuting the existence of CPV in the leptonic sector. In addition to this primary goal, it will also be able to resolve the mass hierarchy and shed light on the octant of θ_{23} . The $\nu_\mu(\bar{\nu}_\mu)$ super-beam will originate at Fermilab. The primary beam simulation assumes a 1.2 MW - 120 GeV proton beam that will deliver 10^{21} protons-on-target (POT) per year. A 35-40 kt Liquid Argon (LAr) far-detector will be housed in the Homestake mine in South Dakota, 1300 km away⁵. The experiment plans to have a total of 10 years of running, divided equally between neutrinos and anti-neutrinos, corresponding to a total exposure of 35×10^{22} kt-POT-yr. Other experimental details, such as signal and background definitions as well as the detector efficiencies taken in this work are the same as those in [60], except with the difference that we have not considered tau events in the backgrounds. We assume a 5% signal normalisation error and a 10% background normalisation error. The detector efficiencies for both $P_{\mu e}$ and $P_{\bar{\mu} \bar{e}}$ events are close to 80% with somewhat less efficiency for $P_{\bar{\mu} \bar{e}}$.

III. RESULTS AND DISCUSSION

A. Sensitivity to CP violation in the presence of a single sterile neutrino

In this section, we show the sensitivities of various long-baseline experiments to leptonic CP violation in the 3+1 scenario. Results for the 3+0 case are provided for comparison. Figs. 1 to 3 show the sensitivity to excluding the CP conserving values as a function of the 3+1 oscillation parameters.

⁵ In addition to this, there is a proposal to install a near detector[64, 65], which among other physics goals can also constrain the parameter space for the 3+1 scenario, as recently discussed in [66]

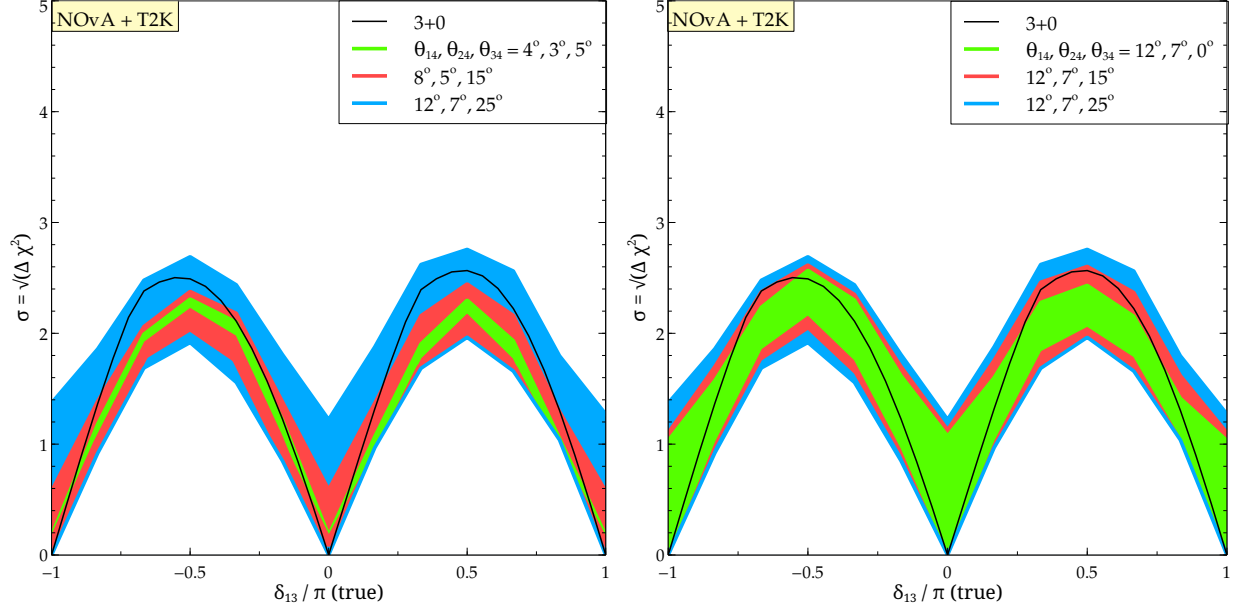


FIG. 1: Sensitivity to CP violation as a function of the true CP violating phase δ_{13} for the combined data from T2K and NO ν A. Different colors correspond to different choice of true $\theta_{14}, \theta_{24}, \theta_{34}$ as shown in the key. Variation of true δ_{24} and δ_{34} results in the colored bands which show the minimum and maximum sensitivity that can be obtained for a particular δ_{13} . The black curve corresponds to sensitivity to CP violation in 3+0. Left panel: Shows the effect as all the three active-sterile mixings are increased. Right panel: Shows the effect of the 3-4 mixing when the true θ_{14} and θ_{24} have been fixed at 12° and 7° respectively for all three bands.

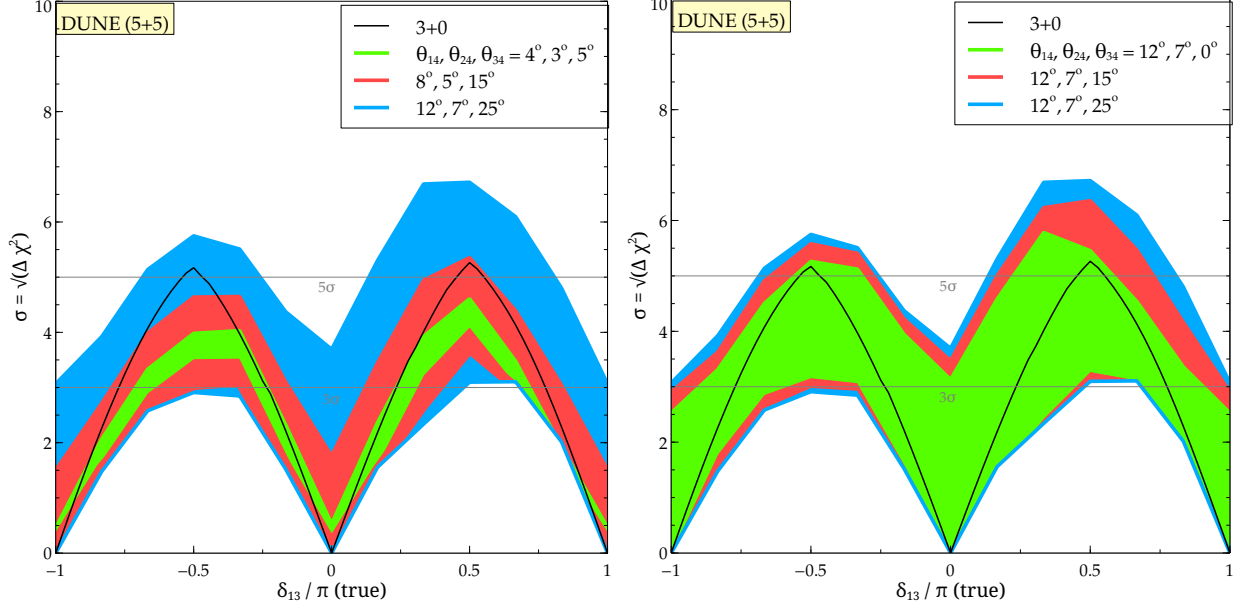


FIG. 2: Similar to Fig. 1 but for DUNE.

We show results for three sets of the active-sterile mixing angles $\theta_{14}, \theta_{24}, \theta_{34}$. These are chosen to be $(4^\circ, 3^\circ, 5^\circ)$, $(8^\circ, 5^\circ, 15^\circ)$ and $(12^\circ, 7^\circ, 25^\circ)$. The *data* are simulated assuming the above three sets of mixing angles and various choices of the three CP phases lying in $[-180^\circ, 180^\circ]$. In the *fit*, we consider the 8 possible CP conserving combinations of $\delta_{13}, \delta_{24}, \delta_{34}$ where each phase could either be 0 or 180° . We minimise the $\Delta\chi^2$ over these 8 test CP conserving cases; and over various test $\theta_{14}, \theta_{24}, \theta_{34}$ samples in the allowed range in the fit, so as to account for the lack of information regarding active-sterile mixings. This gives us a $\Delta\chi^2_{\min}$ as a function of the true parameters. Both for simulating data and in the fit, we assume the hierarchy to be normal only. We did not marginalise over the 3+0 parameters⁶. For a particular true δ_{13} , we show the maximum and the minimum $\Delta\chi^2_{\min}$ that can be obtained corresponding to a variation of the other two true CP phases δ_{24} and δ_{34} . For 3+0, the situation is simpler, where we contrast a true δ_{CP} against $\delta_{\text{CP}} = 0$ and $\delta_{\text{CP}} = \pi$ in the fit.

⁶ Our results show that a close to 5σ determination of hierarchy is very likely with the DUNE experiment, even in the 3+1 paradigm. Among other 3+0 oscillation parameters, marginalisation over θ_{23} may be important when the non-maximal true values like the ones in lower octant or higher octant are considered because of octant-related degeneracies. Since, disappearance ($P_{\mu\mu}$) data fixes $\sin^2 2\theta_{23}$ very accurately, marginalisation over test θ_{23} is not necessary for true $\theta_{23} = 45^\circ$.

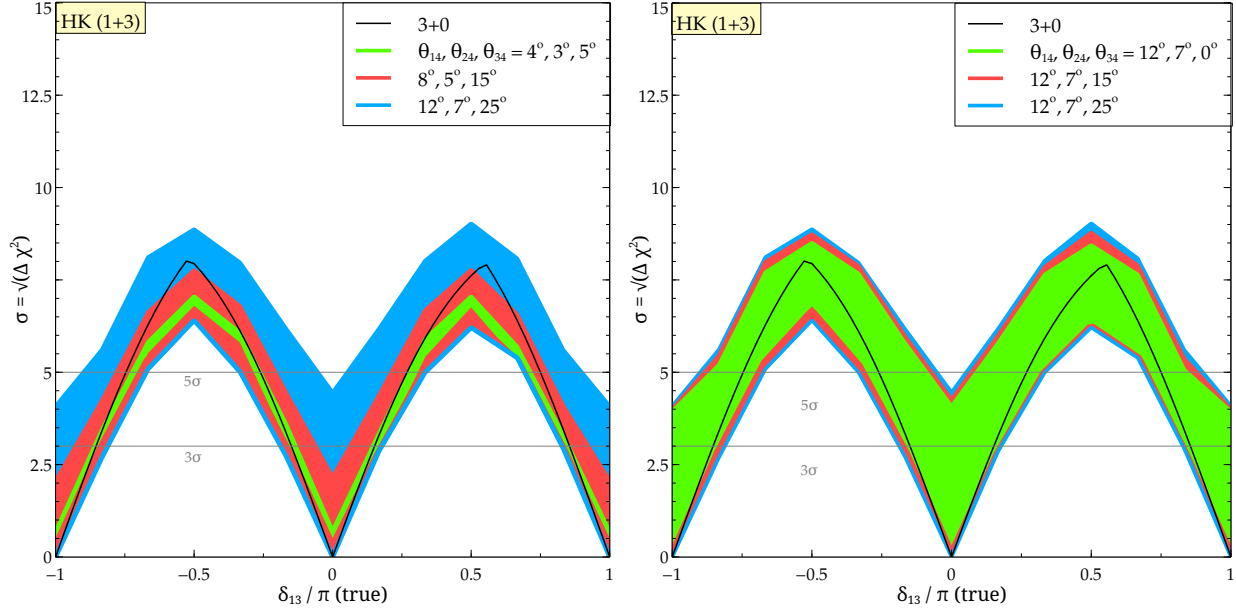


FIG. 3: Similar to Fig. 1 but for T2HK.

It can be seen from Figs. 1 to 3 that the existence of sterile neutrinos can significantly affect the CPV discovery potential of long-baseline experiments. This violation can originate in any of the three phases and not just δ_{13} . When the active-sterile mixings are small, the general trend visible in the figures is that the sensitivity to CP violation of the experiment will be decreased compared to what we would expect in the 3+0 scenario. However, for sufficiently large mixings, the sensitivity spans both sides of the 3+0 curve; and hence, depending on the true value of the other phases - δ_{24} and δ_{34} , the sensitivity to CP violation can be greatly amplified. We observe that the chosen value of true θ_{34} significantly affects the sensitivity to CP violation, especially for DUNE, where the matter effects are large. We also note that there can be significant amplification of CPV sensitivity for regions of δ_{13} where one expects little or none in the 3+0 scenario. Overall, if sterile mixing angles are not tiny, the 3+1 (or 3+n) scenario, if realized in nature, makes the observation of generic CPV *per se* significantly more likely than the 3+0 case, although it makes the determination of the phase (or phases) in which such violation originates much harder (we address this point in greater detail in Subsection III E).

In order to understand the behavior of sensitivities to CP violation and later the mass hierarchy, we note the role of the following competing effects in the calculation of $\Delta\chi_{\min}^2$ ⁷:

⁷ Similar effects can also guide the value of $\Delta\chi_{\min}^2$ in the context of other new physics effects such as NSI and this has been illustrated in [67, 68].

1. The parameter space for the 3+1 scenario consists of $\theta_{14}, \theta_{24}, \theta_{34}, \delta_{24}, \delta_{34}$, and δm_{41}^2 , in addition to the standard 3+0 parameters. While generating the $\Delta\chi_{\min}^2$ curve for 3+0 scenario (black), we marginalized only over the test parameter δ_{13} (*i.e.*, δ_{CP}); however, for the 3+1 curves, marginalization was carried over the five additional test parameters $\theta_{14}, \theta_{24}, \theta_{34}, \delta_{24}, \delta_{34}$ in addition to δ_{13} . Hence, the parameter space for 3+1 case is a substantially larger superset of the 3+0 parameter space. In general, from a statistical point of view, marginalization over a larger space of test parameters tends to bring down the value of $\Delta\chi_{\min}^2$.
2. As the true values of the 3+1 mixing angles $\theta_{14}, \theta_{24}, \theta_{34}$ increase, the impact due to the variation in the true values of the associated phases (δ_{24}, δ_{34}) also increases. This results in substantially broadening the $\Delta\chi_{\min}^2$ bands (for 3+1) in both directions as the true values of $\theta_{14}, \theta_{24}, \theta_{34}$ increase from $4^\circ, 3^\circ, 5^\circ$ to $12^\circ, 7^\circ, 25^\circ$, - thereby making the $\Delta\chi_{\min}^2$ (for 3+1 scenario) sometimes even larger than the 3+0 $\Delta\chi_{\min}^2$.

When the active-sterile mixing angles (true $\theta_{14}, \theta_{24}, \theta_{34}$) are small, effect (2) is small. However, the statistical effect (effect (1) above) stemming from marginalization over five added parameters is significant and reduces the sensitivity in general. Consequently, $\Delta\chi_{\min}^2$ tends to decrease for small values of the true sterile mixing angles. On the other hand, when the mixing angles (true $\theta_{14}, \theta_{24}, \theta_{34}$) increase, they concurrently amplify the effect of the CP violating phases. Consequently, effect (2) plays a correspondingly important role, and tends to increase $\Delta\chi_{\min}^2$ overall. These features have been explained in greater detail in Subsection [III C](#) using the DUNE total neutrino and anti-neutrino event rates as an example.

B. Mass hierarchy

In this section, we re-evaluate the sensitivities of the long-baseline experiments to the neutrino mass hierarchy, assuming the 3+1 scenario. We show results assuming the normal hierarchy. The simulation procedure followed here is the same as that described in Sec. [III A](#) except for the following important differences:

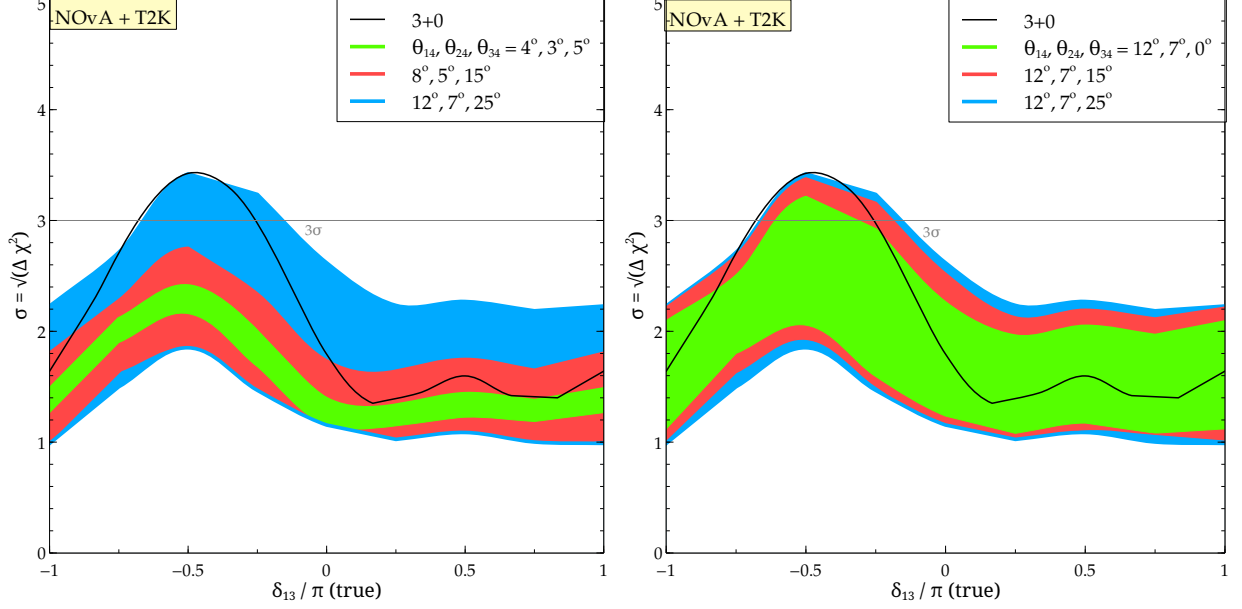


FIG. 4: Sensitivity to Mass hierarchy as a function of the true CP violating phase δ_{13} for the combined data from T2K and NO ν A. Different colors correspond to different choice of true $\theta_{14}, \theta_{24}, \theta_{34}$ as shown in the key. Variation of true δ_{24} and δ_{34} results in the colored bands which show the minimum and maximum sensitivity that can be obtained for a particular δ_{13} . The black curve corresponds to sensitivity to the hierarchy in 3+0. Left panel: Shows the effect as all the three active-sterile mixings are increased. Right panel: Shows the effect of the 3-4 mixing when the true θ_{14} and θ_{24} have been fixed at 12° and 7° respectively for all three bands.

- In the fit, we assume the hierarchy to be inverted.
- For the CP violation sensitivities, in the fit, we had considered only those combinations of test values of $\delta_{13}, \delta_{24}, \delta_{34}$ which were CP conserving. For hierarchy determination, however, we have varied these test CP phases in their full allowed range $[-180^\circ, 180^\circ]$ and have marginalised over them.

Note that, as in the previous section, we did not vary the test 3+0 parameters in the fit. We show the results in Figs. 4 and 5 as a function of the true 3+1 parameters. For the combined results from T2K and NO ν A, it can be seen in Fig. 4 (left panel) that there emerges the possibility of significant improvement in the hierarchy sensitivity compared to 3+0 (shown by black line) in the unfavourable regions of true δ_{13} . The extent of this enhancement is, of course, dependent on the true values of the active-sterile oscillation parameters. Fig. 4

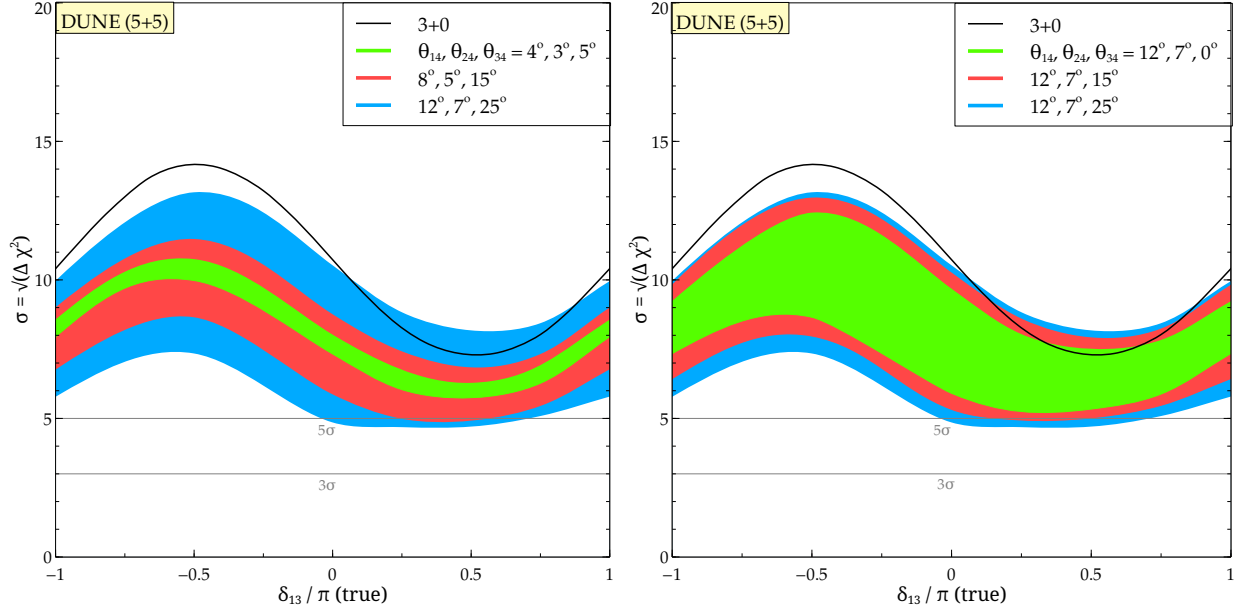


FIG. 5: Similar to Fig. 4 but for DUNE.

(right panel) shows the dependence of sensitivity on the θ_{34} mixing angle - the effects of which are noticeable, although not large, even for baselines where matter effects are not very substantial.

In the case of DUNE, we find that the 3+1 sensitivities are usually below 3+0 sensitivities⁸ except for a small region of parameter space around true $\delta_{13} = 90^\circ$, as can be observed in both the panels of Fig. 5. The θ_{34} -dependence of sensitivities is somewhat more pronounced for DUNE, as is evident from the right panel of Fig. 5. It should be noted that except for a small fraction of parameter space around true $\delta_{13} = 90^\circ$, the sensitivity stays above 5σ C.L.

⁸ As mentioned in the beginning of the present subsection III B, the test CP phases have been marginalized over their full allowed range $[-180^\circ, 180^\circ]$ while calculating the $\Delta\chi_{\min}^2$ for mass hierarchy; whereas for CP violation sensitivity the marginalization was carried over the CP violating values - 0° and 180° only. This enhanced range of marginalization for mass hierarchy leads to a larger statistical effect (see effect (1) in the previous subsection), leading to a generally reduced $\Delta\chi_{\min}^2$ for 3+1, compared to the 3+0 case.

C. Using total event rates to understand the DUNE sensitivity to Hierarchy and CPV

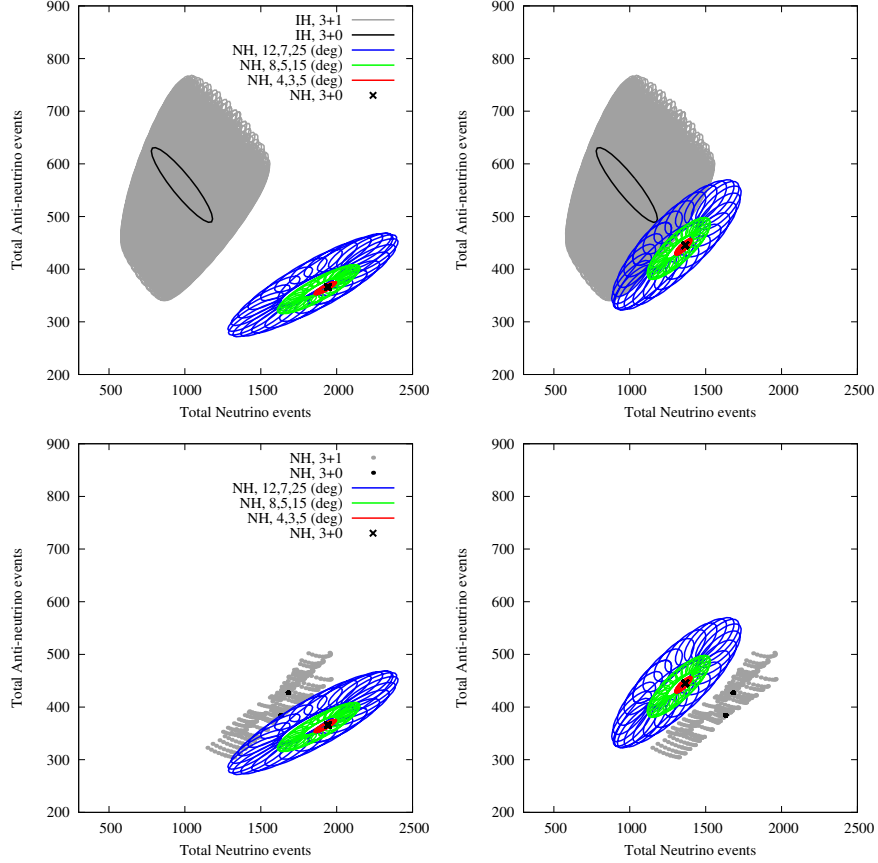


FIG. 6: Neutrino and Anti-neutrino event rates for the DUNE experiment. The top panels are to explain the observed hierarchy sensitivity while the bottom panels are for CPV. The event rates in blue, green and red correspond to the simulated data with NH and the active-sterile mixings as depicted in the keys. The black cross corresponds to events for NH and $\delta_{CP} = -90^\circ$ (90°) assuming 3+0 for the left (right) panel. The event rates in grey in the top panel correspond to the fit events rates assuming 3+1 where all the active-sterile oscillation parameters have been varied. The event rates in grey in the bottom panel correspond to fit event rates assuming 3+1 where the active-sterile mixing angles have been varied and each of the three CP phases is either 0 or π . In the top (bottom) panels, the assumed hierarchy for fit events is IH (NH). In the top panels, the black ellipses correspond to fit events with only δ_{CP} varied assuming 3+0. In the bottom panels, the black dots correspond to fit events with $\delta_{CP} = 0, \pi$ assuming 3+0.

This subsection attempts to obtain a better understanding of the changes that occur in CP and hierarchy sensitivities at long baselines (as seen in subsections III A and III B) in the presence of a sterile neutrino. It provides, in effect, an alternative way of looking at the qualitative behaviour exhibited by the sensitivities in Figs. 1 through 5 and complements the discussion in the subsections above. We use DUNE as our primary example, but the features discussed below are, in general, displayed in the figures corresponding to other experiments as well, *e.g.* those for NOvA + T2K or for HK.

In Fig. 6, we try to explain the results that we obtained for the hierarchy and CP violation sensitivities of the DUNE experiment using total (energy-integrated) neutrino and anti-neutrino event rates. The top panels of Fig. 6 refer to the hierarchy sensitivity behavior while the bottom panels are for CP violation. The regions shown in red, green, blue and the black cross correspond to true oscillation parameters (or the data). The regions in grey, the black dots and the black ellipses correspond to the test oscillation parameters (or the fit).

The data events on the left plots are for true NH and true $\delta_{13} = -90^\circ$ while the data events on the right plots are for true NH and true $\delta_{13} = 90^\circ$. The grey fit events in the top panels correspond to test IH and all 3+1 ($\theta_{14}, \theta_{24}, \theta_{34}, \delta_{24}, \delta_{34}$ in addition to δ_{13}) parameters varied, while the black ellipse in the top panel corresponds to test IH and variation of δ_{CP} only. The grey fit events in the bottom panel correspond to test NH and test CP-conserving combinations of δ_{24}, δ_{34} , while the black dots in the bottom panel corresponds to test NH and test $\delta_{CP} = 0, \pi$. The event numbers corresponding to 3+0 have been shown using black ellipses, black dots and black crosses. Broadly, it can be said that the sensitivities will be better if the data events and the fit events are well separated (ignoring sensitivity coming from spectral information). The sensitivity patterns can be understood if we focus on the following two features:

- The fit event rates region increases drastically as we go from 3+0 to 3+1 (black ellipses and dots compared to grey regions). Note that we marginalise over the entire allowed 3+1 oscillation parameter space.
- For small mixing angles θ_{i4} , the event rate regions are small compared to their size for large mixing angles (red compared to green and blue).

Thus, we can make the following deductions which are reflected in the sensitivity plots.

- Compared to 3+0, the 3+1-small mixing angles reduce the sensitivity of DUNE to hierarchy or CP violation because although the increase in the data event regions is small, the fit event regions cover significantly more area, decreasing the separation between the two types of regions, and consequently, the sensitivity. This is visible in the green regions in the left panels of Figs. 2 and 5.
- As we go from small mixing angles to large mixing angles, the area covered by the data event rates increases significantly. Thus, there are oscillation parameters for which the data events are either very far or very close to the fit event regions compared to 3+0. Consequently, the 3+1 sensitivities can be much better or much worse compared to the 3+0. This is demonstrated, for instance, by the blue regions in the left panels of Fig. 2 (both better and worse; for CP) and Fig. 5 (mostly worse; for hierarchy).
- Fig. 6 also makes it easier to understand the behavior with respect to true δ_{13} . As we go from $\delta_{13} = -90^\circ$ (left plots) to $\delta_{13} = 90^\circ$ (right plots), the fit rates approach data rates in the case of hierarchy and hence the sensitivity decreases, as seen in the coloured regions of both the left and right panels of Fig. 5. However, in the case of CP violation, the fit rates are symmetrically placed around the data region and therefore, the sensitivity remains roughly the same in both quadrants, as is manifested in the left and right panels of Fig. 2.

D. To what extent can DUNE ignore the presence of the 3+1 sector if it is present?

In this subsection we explore the question whether the CP-related measurements at DUNE can get affected by assuming the absence of sterile neutrinos when they exist in reality, but are obscure because of very small mixings. To explore this point in greater detail, we carry out the following exercise. We assume that the true scenario is 3+1 with sufficiently small active-sterile mixings such that $\sin^2 2\theta_{\mu e} \leq 10^{-3}$, *i.e.* below the currently stated sensitivity of short-baseline experiments planned or underway at Fermilab [32–35]. For such small values of θ_{14} and θ_{24} , θ_{34} is rendered inconsequential in $P_{\mu e}$; therefore, we assume $\theta_{34} = \delta_{34} = 0$ for simplicity. We choose several true values of δ_{13} and $\delta_{24} \in [-180^\circ, 180^\circ]$. In the fit, we assume 3+0 and vary $\delta_{\text{CP}} \in [-180^\circ, 180^\circ]$, calculating the sensitivity at each test δ_{CP} . We fix the remaining 3+0 oscillation parameters in the fit at their true values.

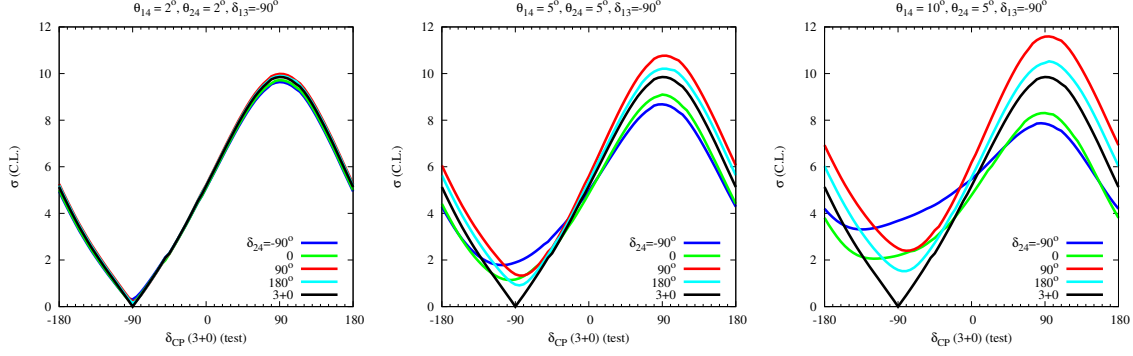


FIG. 7: $\sigma = \sqrt{\Delta\chi^2}$ as a function of test δ_{CP} for the DUNE experiment. We contrast 3+1 as the true case with 3+0 as the test case. Results are shown for different 3+1 oscillation parameters. These plots are for true $\delta_{13} = -90^\circ$. True δ_{24} values have been varied as shown in the key. The left, middle and right panels correspond to true $\theta_{14} = \theta_{24} = 2^\circ$, $\theta_{14} = \theta_{24} = 5^\circ$ and $\theta_{14} = 10^\circ, \theta_{24} = 5^\circ$ (*i.e.* $\sin^2 2\theta_{\mu e}$ equal to 6×10^{-6} , 2×10^{-4} and 9×10^{-4}) respectively. We assume $\theta_{34} = \delta_{34} = 0$. Both true as well as test hierarchy is assumed to be normal. The black curve shows the usual sensitivity when both true and test are 3+0.

The results are shown in Fig. 7, and the details of our assumptions and chosen values are as described in the figure caption.

It is possible to obtain the following information from the curves in Fig. 7:

- They show the allowed test δ_{CP} region. For example, in the 3+0 scenario, DUNE should be able to measure δ_{CP} with a precision of $\pm 60^\circ$ at 3σ C.L. if true $\delta_{\text{CP}} = -90^\circ$.
- They demonstrate the sensitivity at which the experiment can exclude CP conservation *i.e.* test $\delta_{\text{CP}} = 0, 180^\circ$ if the true $\delta_{\text{CP}} = -90^\circ$.
- Finally, they help answer the question: Can 3+0 be excluded if 3+1 is true? If for all test δ_{CP} values, $\Delta\chi^2 > N^2$, then we can say that 3+0 can be excluded at $N\sigma$.

We observe in Fig. 7 that if θ_{14} and θ_{24} are as small as 2° each (left panel), then the results obtained are essentially the same even if the wrong theoretical framework of 3+0 is considered while fitting the data. For angles as large as 5° (middle panel), there are visible but not highly significant deviations from the 3+0 results. Depending on the true value of δ_{24} , the precision with which DUNE measures δ_{13} can improve or worsen by $\sim 10^\circ$. However, the predicted best fit is around the right test δ_{CP} ($= -90^\circ$) in most cases. An offset, of $\sim 15^\circ$, is obtained depending on the true value of δ_{24} . For the 3+0 case, DUNE can

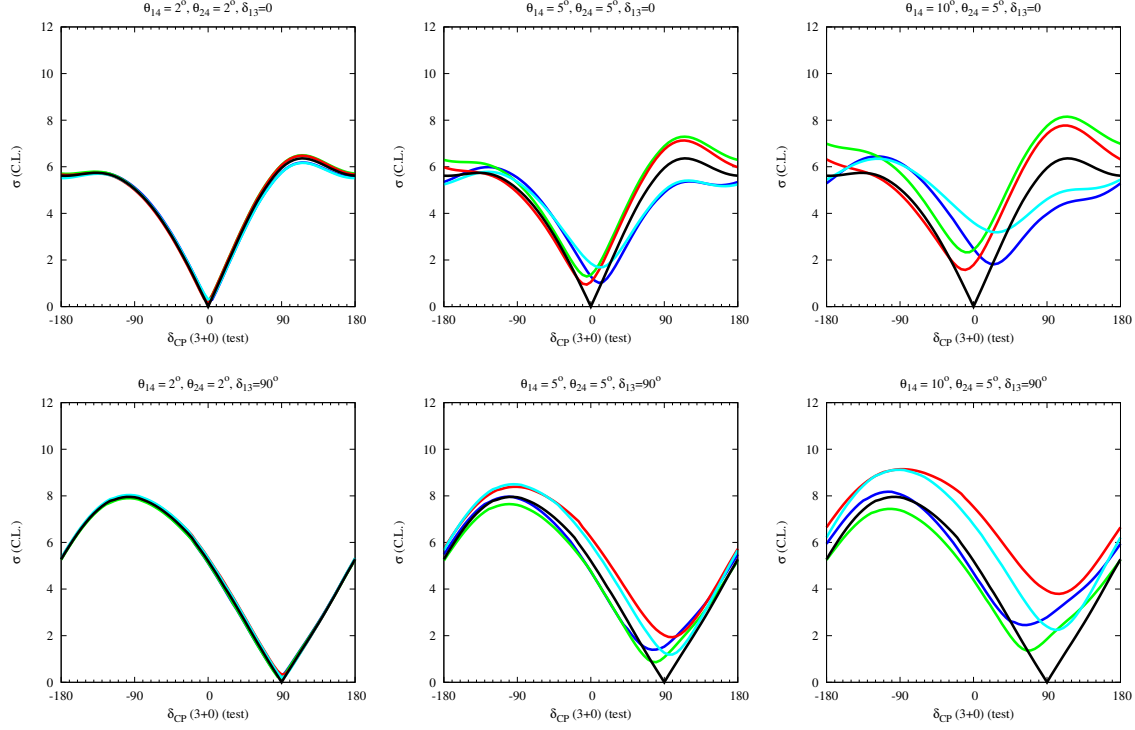


FIG. 8: Same as Fig. 7, but for $\delta_{13} = 0$ (top panel) and $\delta_{13} = 90^\circ$ (bottom panel).

exclude CP conserving test $\delta_{\text{CP}} = -180^\circ$ at 5σ . This sensitivity, in the 3+1 case, can vary from $4\text{--}6\sigma$. For $\theta_{14} = \theta_{24} = 5^\circ$, DUNE can exclude 3+0 at $1\text{--}2\sigma$ depending on the true value of δ_{24} . For still larger values of mixing angles like $\theta_{14} = 10^\circ, \theta_{24} = 5^\circ$, we observe similar features except that the $\Delta\chi^2$ are larger i.e. DUNE is more likely to exclude 3+0.

This exercise has been repeated for true $\delta_{13} = 0$ and 90° in Fig. 8, with similar results.

E. Determining the δ phase responsible for CP violation in 3+1

Suppose that the results of short-baseline experiments indicate the presence of a ~ 1 eV neutrino, and, in addition, DUNE finds evidence of CP violation. Assuming this situation, we attempt to examine the extent and accuracy with which DUNE can identify the source of this violation, *i.e.* the particular 3+1 phase (*i.e.* δ_{13} , δ_{24} or δ_{34}) associated with it. To simplify matters, we assume near-maximal-allowed values of the sterile mixing angles; *i.e.* $(\theta_{14}, \theta_{24}, \theta_{34}) : (12^\circ, 7^\circ, 25^\circ)$ and also fix the true value of δ_{34} to 0, in order to better bring out the effect of the other two CP phases.

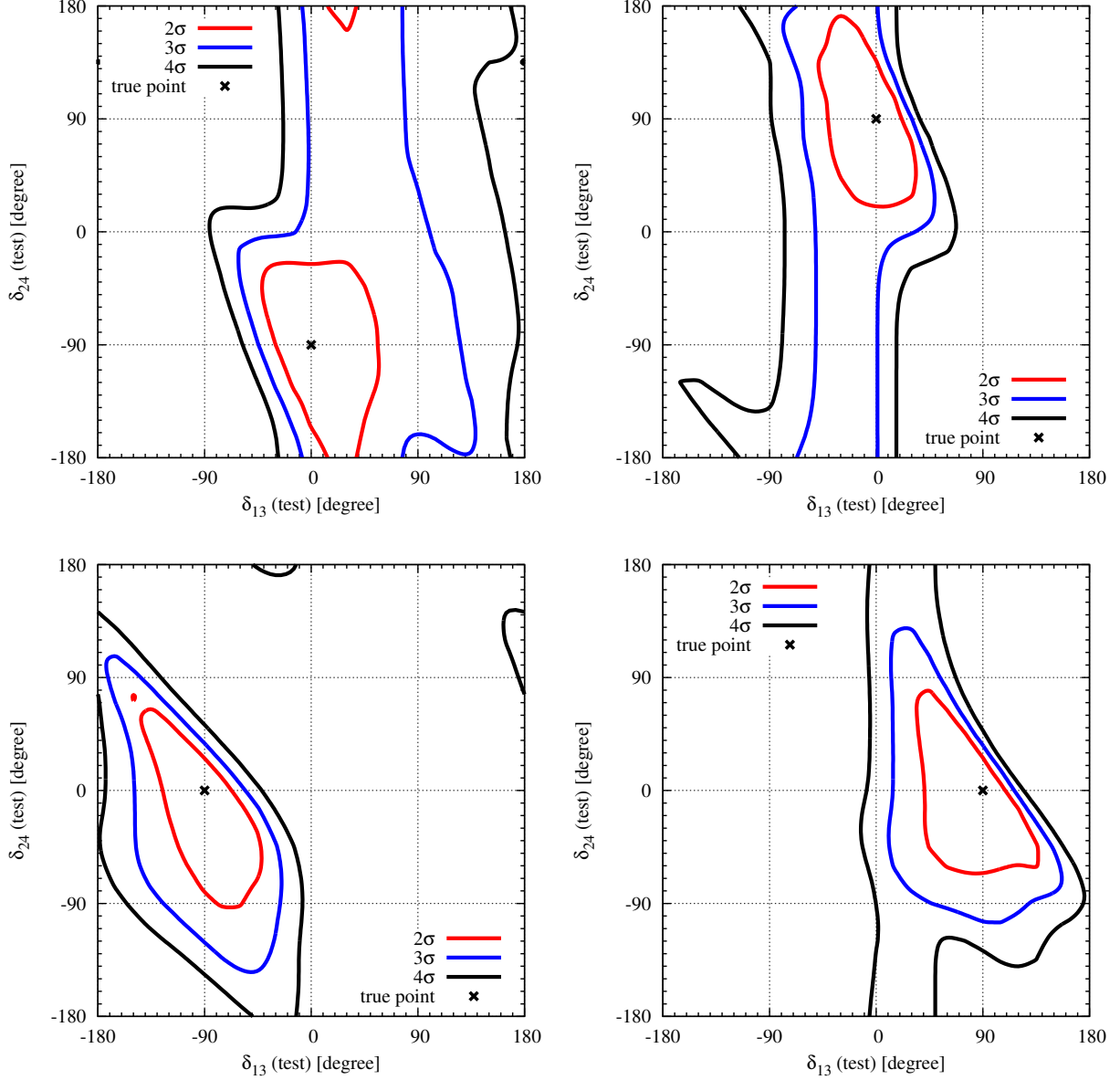


FIG. 9: The allowed-region contours in the test δ_{13} - test δ_{24} plane for DUNE. True $(\theta_{14}, \theta_{24}, \theta_{34})$ were taken to be $(12^\circ, 7^\circ, 25^\circ)$ and true $\delta_{34} = 0$. Results have been shown for true $(\delta_{13}, \delta_{24}) = (0, \pm 90^\circ)$ and $(\pm 90^\circ, 0)$. 2σ , 3σ , and 4σ results (corresponding to $\Delta\chi^2_{\min} = 6.18, 11.83$ and 19.33 respectively for two degrees of freedom) have been shown. The true point in each plot has been shown with a cross.

Results are shown for the following four combinations of true $(\delta_{13}, \delta_{24})$: $(0, \pm 90^\circ)$ and $(\pm 90^\circ, 0)$. These correspond to the situation where one of the phases is maximally CP violating, while the other is CP conserving. In the fit, we marginalised over the test active-sterile mixing angles and the test CP phase δ_{34} . The 2σ , 3σ and 4σ allowed regions in the

test δ_{13} - test δ_{24} plane are shown in Fig. 9 for the above-mentioned four true combinations (these plots can also be used to find out the precision with which DUNE can measure the CP phases; see [44, 46] for such results).

The top panels of Fig. 9 correspond to the choice of true $(\delta_{13}, \delta_{24})$ being $(0, -90^\circ)$ (left) and $(0, 90^\circ)$ (right). In the left panel, we see that test values of $(\delta_{13}, \delta_{24})$ close to $(90^\circ, 0)$ and $(90^\circ, -180^\circ)$ are allowed within 3σ contours. Thus, it might be concluded that attributing CP violation unambiguously to δ_{24} may not be possible at 3σ . In the right panel, we see that test $(\delta_{13}, \delta_{24})$ close to $(-90^\circ, 0)$ and $(-90^\circ, 180^\circ)$ are allowed, but at 4σ . Similar conclusions can also be drawn for the plots in the bottom panel where distinguishing maximally CP-violating δ_{13} and CP conserving δ_{24} from maximally CP-violating δ_{24} and CP conserving δ_{13} may not be possible at 4σ .

F. How large do active-sterile mixings need to be before DUNE becomes sensitive to their presence?

The Short Baseline Neutrino (SBN) program at Fermilab aims to conclusively establish the existence or else to place stringent constraints on the possible existence of the sterile neutrinos. At short baselines, the $P_{\mu e}$ oscillation probability is sensitive only to the mass-squared difference δm_{41}^2 and an effective mixing angle given by $\sin^2 2\theta_{\mu e} = \sin^2 2\theta_{14} \sin^2 \theta_{24}$. For $\delta m_{41}^2 \sim 1 \text{ eV}^2$ induced oscillations, the SBN program can exclude at 3σ only $\sin^2 2\theta_{\mu e} \geq 0.001$ [35]. It is natural to ask how tightly active-sterile mixings need to be excluded to ensure that DUNE measurements can be safely interpreted without taking the possible existence of sterile neutrinos into account. Phrasing this question another way, we ask whether active-sterile mixings corresponding to $\sin^2 2\theta_{\mu e} < 0.001$ can be detected by the DUNE far detector. Fig. 10 (left panel) throws some light on this question. Here, we have compared the CP bands in event rates assuming 3+1 and 3+0 for very small mixing angles - $\theta_{14}, \theta_{24}, \theta_{34} = 3^\circ, 2^\circ, 10^\circ$ ($\sin^2 2\theta_{\mu e} \approx 0.00001$). We see that the 3+1 band is completely degenerate with the 3+0 band (incorporating the errorbars⁹). Thus, for such small mixing angles, it seems that neither the Short Baseline experiments nor the DUNE experiment may see evidence of new physics attributable to sterile neutrinos. In the right panel of the same

⁹ The error for each energy bin is the quadrature sum of the statistical ($\sqrt{\text{Event no.}}$) and the systematic error (2%)[69]. The value is an estimated expected value assuming the presence of a highly capable near-detector[69].

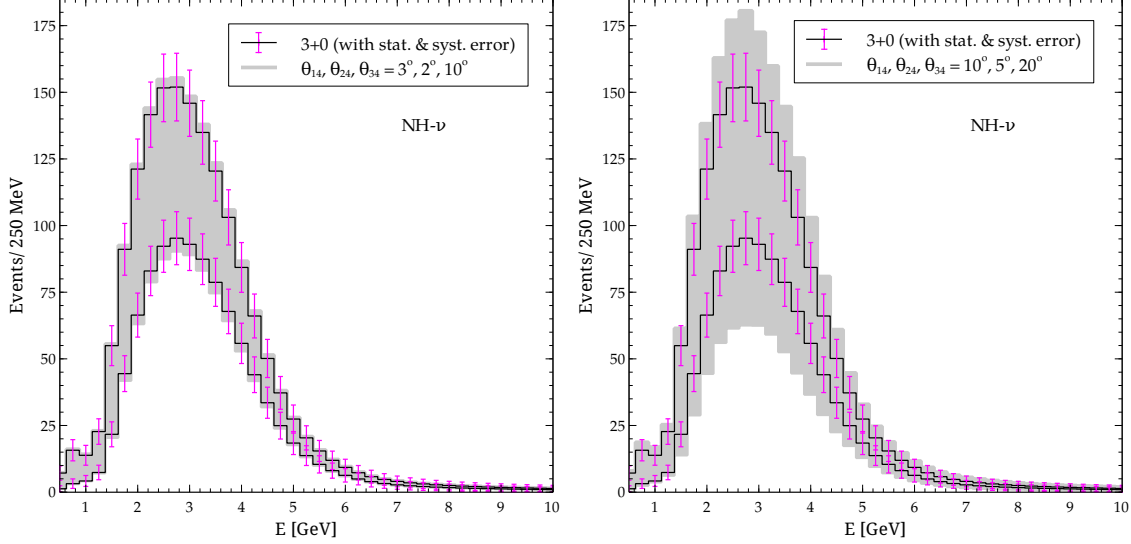


FIG. 10: Neutrino event rates for the DUNE experiment as a function of the reconstructed neutrino energy. The black lines show the maximum and the minimum event rates corresponding to a variation of δ_{CP} in 3+0. Also shown are the corresponding statistical ($\sqrt{\text{Event no.}}$) and systematic error (2%) [69] added in quadrature for each energy bin. The grey band corresponds to the maximum and minimum event rates assuming 3+1 with $\theta_{14}, \theta_{24}, \theta_{34} = 3^\circ, 2^\circ, 10^\circ$ (left panel), $\theta_{14}, \theta_{24}, \theta_{34} = 10^\circ, 5^\circ, 20^\circ$ (right panel) and $\delta_{13}, \delta_{24}, \delta_{34}$ varied in $[-180^\circ, 180^\circ]$. Only the channel $\nu_\mu \rightarrow \nu_e$ has been considered with 5 years of ν -running assuming normal hierarchy.

figure, however, we have chosen $\theta_{14}, \theta_{24}, \theta_{34} = 10^\circ, 5^\circ, 20^\circ$ ($\sin^2 2\theta_{\mu e} \approx 0.0009$). These larger values, which correspond to an effective mixing angle at the 3σ sensitivity of the short-baseline experiments, lead to enhanced effects. The grey band now extends significantly beyond the expected event rates for 3+0, even after accounting for errors. This provides a suggestive estimate of how large the mixing angles need to be before sterile neutrino effects at DUNE start to be discernable.

We stress that short-baseline experiments are significantly more sensitive, by design, to CP conserving oscillatory effects in 3+1 compared to long-baseline experiments, and hence remain the definitive test by which presence or absence of sterile neutrinos can be established. Long-baseline experiments, however, can become sensitive to the presence of this sector if CPV is present. Moreover, matter enhances the effects of CP, further enabling these experiments to become, in a sense, complementary detectors of sterile neutrinos [27]. Signals that could possibly be interpreted as those for sterile neutrinos at long-baseline

experiments like DUNE would, however, remain supportive rather than definitive evidence, because they could conceivably be mimicked by other physics beyond the SM (see, for instance, [67, 68, 70–80] for the effect of propagation NSI on long baselines, especially at DUNE in the context of CP Violation and Mass hierarchy.).

IV. CONCLUSIONS AND SUMMARY

This work examines how sensitivities of long-baseline experiments to the MH and CP violation are affected and altered in the presence of a sterile neutrino. It attempts to quantitatively examine questions raised in [27]. While we use DUNE as our benchmark example, we study these sensitivities for T2K, HK, and NOvA also. Depending on the values of sterile mixing angles and phases, the sensitivities can be both significantly enhanced or suppressed compared to the 3+0 case. We examine and discuss the reasons for this behaviour using the total event rate as a tool.

We also examine the ability of DUNE to pinpoint the origin of CPV, if such violation is detected by it. We find that while the discovery potential for the violation is large, determining its origin (*i.e.* ascribing it unambiguously to either the 3+0 phase δ_{CP} or one of the other phases δ_{24} , δ_{34} , present in 3+1) is much more challenging. Indeed, 3σ determination of the phase (or phases) responsible for CPV could prove very elusive both if sterile neutrinos are shown to exist, or if their existence cannot be conclusively ruled out by the short-baseline experiments. If the latter is the case, we ask how tightly one must then bound the sterile-active mixing angles to ensure that DUNE data can be safely interpreted without taking the possible existence of sterile neutrinos into account. In the process, we find that DUNE may exhibit signals hinting at the presence of a sterile sector even if the relevant mixing angles lie below the sensitivity of the planned short-baseline experiments. However, the ability of long-baseline efforts like DUNE to signal the presence of this sector, while highly valuable, must remain complementary to an essential and primary short-baseline thrust aimed at discovering evidence of short-wavelength oscillations with convincing redundancy. As emphasized both in [27] and this work, the sensitivity of DUNE to sterile neutrinos has qualitatively different origins and depends on interference effects and the matter enhancement of the corresponding mixing angles and CP violating phases. These are certainly aspects which do not lie within the physics ambit of short-baseline experiments; however, the resulting signals could also be

mimicked by other new physics, preventing their unambiguous interpretation if considered in isolation.

In summary, DUNE provides strong and valuable complementarity in the search for a sterile sector to be conducted by the short-baseline experiments. It would be useful, in our view, to incorporate this capability into the thinking and efforts currently underway towards optimizing its design.

ACKNOWLEDGMENTS

We gratefully acknowledge many helpful discussions on DUNE fluxes and errors with Mary Bishai and Elizabeth Worcester. We are also thankful to Dan Cherdack, Georgia Karagiorgi, Bryce Littlejohn, Poonam Mehta and Lisa Whitehead for very useful discussions. We also acknowledge the use of the HPC cluster facility at HRI for carrying out the numerical computations used in this work. RG acknowledges support and hospitality from the Neutrino and Theory Divisions at Fermilab while this work was in progress. DD, RG and MM acknowledge support from the DAE Neutrino project at HRI. Fermilab is operated by Fermi Research Alliance, LLC under contract no. DE-AC02-07CH11359 with the US Department of Energy.

-
- [1] Z. Maki, M. Nakagawa, and S. Sakata, Prog. Theor. Phys. **28**, 870 (1962).
 - [2] B. Pontecorvo, Sov. Phys. JETP **26**, 984 (1968), [Zh. Eksp. Teor. Fiz.53,1717(1967)].
 - [3] V. N. Gribov and B. Pontecorvo, Phys. Lett. **B28**, 493 (1969).
 - [4] Y. Ashie et al. (Super-Kamiokande), Phys. Rev. Lett. **93**, 101801 (2004), hep-ex/0404034.
 - [5] R. Wendell et al. (Super-Kamiokande), Phys. Rev. **D81**, 092004 (2010), 1002.3471.
 - [6] B. Aharmim et al. (SNO), Phys. Rev. **C72**, 055502 (2005), nucl-ex/0502021.
 - [7] M. H. Ahn et al. (K2K), Phys. Rev. **D74**, 072003 (2006), hep-ex/0606032.
 - [8] D. G. Michael et al. (MINOS), Phys. Rev. Lett. **97**, 191801 (2006), hep-ex/0607088.
 - [9] P. Adamson et al. (MINOS), Phys. Rev. **D77**, 072002 (2008), 0711.0769.
 - [10] K. Abe et al. (T2K), Phys. Rev. Lett. **112**, 061802 (2014), 1311.4750.
 - [11] K. Abe et al. (T2K), Phys. Rev. Lett. **112**, 181801 (2014), 1403.1532.

- [12] T. Araki et al. (KamLAND), Phys. Rev. Lett. **94**, 081801 (2005), hep-ex/0406035.
- [13] C. Arpesella et al. (Borexino), Phys. Rev. Lett. **101**, 091302 (2008), 0805.3843.
- [14] F. P. An et al. (Daya Bay), Phys. Rev. Lett. **108**, 171803 (2012), 1203.1669.
- [15] J. K. Ahn et al. (RENO), Phys. Rev. Lett. **108**, 191802 (2012), 1204.0626.
- [16] Y. Abe et al. (Double Chooz), Phys. Rev. **D86**, 052008 (2012), 1207.6632.
- [17] G. L. Fogli, E. Lisi, A. Marrone, D. Montanino, A. Palazzo, and A. M. Rotunno, Phys. Rev. **D86**, 013012 (2012), 1205.5254.
- [18] M. C. Gonzalez-Garcia, M. Maltoni, and T. Schwetz (2015), 1512.06856.
- [19] D. V. Forero, M. Tortola, and J. W. F. Valle, Phys. Rev. **D90**, 093006 (2014), 1405.7540.
- [20] G. Altarelli, Int. J. Mod. Phys. **A29**, 1444002 (2014), 1404.3859.
- [21] A. Aguilar-Arevalo et al. (LSND), Phys.Rev. **D64**, 112007 (2001), hep-ex/0104049.
- [22] A. Aguilar-Arevalo et al. (MiniBooNE), Phys.Rev.Lett. **102**, 101802 (2009), 0812.2243.
- [23] G. Mention, M. Fechner, T. Lasserre, T. Mueller, D. Lhuillier, et al., Phys.Rev. **D83**, 073006 (2011), 1101.2755.
- [24] T. Mueller, D. Lhuillier, M. Fallot, A. Letourneau, S. Cormon, et al., Phys.Rev. **C83**, 054615 (2011), 1101.2663.
- [25] A. Aguilar-Arevalo et al. (MiniBooNE), Phys.Rev.Lett. **110**, 161801 (2013), 1207.4809.
- [26] N. Klop and A. Palazzo, Phys. Rev. **D91**, 073017 (2015), 1412.7524.
- [27] R. Gandhi, B. Kayser, M. Masud, and S. Prakash, JHEP **11**, 039 (2015), 1508.06275.
- [28] D. S. Ayres et al. (NOvA) (2007).
- [29] *Fundamental Physics at the Intensity Frontier* (2012), 1205.2671, URL <https://inspirehep.net/record/1114323/files/arXiv:1205.2671.pdf>.
- [30] C. Adams et al. (LBNE) (2013), 1307.7335, URL <http://www.osti.gov/scitech/biblio/1128102>.
- [31] K. Abe et al. (Hyper-Kamiokande Proto-Collaboration), PTEP **2015**, 053C02 (2015), 1502.05199.
- [32] M. Antonello et al. (LAr1-ND, ICARUS-WA104, MicroBooNE) (2015), 1503.01520.
- [33] Joseph Zennamo, 48th Annual Fermilab User's Meeting (June 2015), URL <https://indico.fnal.gov/getFile.py/access?contribId=54&sessionId=23&resId=0&materialId=slides&confId=8982>.
- [34] Diego Garcia-Gamez, The University of Manchester (2016), URL <http://indico>.

- hep.manchester.ac.uk/getFile.py/access?contribId=156&sessionId=6&resId=0&materialId=slides&confId=4534.
- [35] L. Camilleri, AIP Conference Proceedings **1680**, 020004 (2015), URL <http://scitation.aip.org/content/aip/proceeding/aipcp/10.1063/1.4931863>.
 - [36] A. Donini, M. Lusignoli, and D. Meloni, Nucl.Phys. **B624**, 405 (2002), hep-ph/0107231.
 - [37] A. Dighe and S. Ray, Phys.Rev. **D76**, 113001 (2007), 0709.0383.
 - [38] A. Donini, K.-i. Fuki, J. Lopez-Pavon, D. Meloni, and O. Yasuda, JHEP **0908**, 041 (2009), 0812.3703.
 - [39] O. Yasuda, pp. 300–313 (2010), 1004.2388.
 - [40] D. Meloni, J. Tang, and W. Winter, Phys.Rev. **D82**, 093008 (2010), 1007.2419.
 - [41] B. Bhattacharya, A. M. Thalappilil, and C. E. Wagner, Phys.Rev. **D85**, 073004 (2012), 1111.4225.
 - [42] P. Adamson et al. (MINOS), Phys.Rev.Lett. **112**, 191801 (2014), 1403.0867.
 - [43] D. Hollander and I. Mocioiu, Phys.Rev. **D91**, 013002 (2015), 1408.1749.
 - [44] J. M. Berryman, A. de Gouvea, K. J. Kelly, and A. Kobach, Phys. Rev. **D92**, 073012 (2015), 1507.03986.
 - [45] S. K. Agarwalla, S. S. Chatterjee, A. Dasgupta, and A. Palazzo, JHEP **02**, 111 (2016), 1601.05995.
 - [46] S. K. Agarwalla, S. S. Chatterjee, and A. Palazzo (2016), 1603.03759.
 - [47] M. A. Acero, A. A. Aguilar-Arevalo, and J. C. D’Olivo, Journal of Physics: Conference Series **315**, 012015 (2011), URL <http://stacks.iop.org/1742-6596/315/i=1/a=012015>.
 - [48] P. Huber, M. Lindner, and W. Winter, Comput.Phys.Commun. **167**, 195 (2005), hep-ph/0407333.
 - [49] P. Huber, J. Kopp, M. Lindner, M. Rolinec, and W. Winter, Comput. Phys. Commun. **177**, 432 (2007), hep-ph/0701187.
 - [50] J. Kopp, Sterile neutrinos and non-standard neutrino interactions in GLoBES, November 2010. <https://www.mpi-hd.mpg.de/personalhomes/globes/tools/snu-1.0.pdf> (2010).
 - [51] J. Kopp, M. Lindner, T. Ota, and J. Sato, Phys. Rev. **D77**, 013007 (2008), 0708.0152.
 - [52] M. Gonzalez-Garcia, M. Maltoni, and T. Schwetz, JHEP **1411**, 052 (2014), 1409.5439.
 - [53] F. Capozzi, G. Fogli, E. Lisi, A. Marrone, D. Montanino, et al., Phys.Rev. **D89**, 093018 (2014), 1312.2878.

- [54] A. Esmaili, E. Kemp, O. Peres, and Z. Tabrizi, Phys.Rev. **D88**, 073012 (2013), 1308.6218.
- [55] J. Kopp, P. A. N. Machado, M. Maltoni, and T. Schwetz, JHEP **1305**, 050 (2013), 1303.3011.
- [56] F. P. An et al. (Daya Bay), Phys. Rev. Lett. **113**, 141802 (2014), 1407.7259.
- [57] Y. Declais et al., Nucl. Phys. **B434**, 503 (1995).
- [58] B. Jones, *Results of the Search for Sterile Neutrinos with IceCube*, talk at FermiLab, February 12, 2016. "<https://hep.uchicago.edu/seminars/semwin2016/BenJones1.pdf>" (2016).
- [59] P. Adamson et al. (MINOS), Phys. Rev. Lett. **107**, 011802 (2011), 1104.3922.
- [60] M. Bass et al., Phys. Rev. **D91**, 052015 (2015), 1311.0212.
- [61] Y. Itow et al. (T2K), in *Neutrino oscillations and their origin. Proceedings, 3rd International Workshop, NOON 2001, Kashiwa, Tokyo, Japan, December 508, 2001* (2001), pp. 239–248, hep-ex/0106019, URL <http://alice.cern.ch/format/showfull?sysnb=2258620>.
- [62] M. Ishitsuka, T. Kajita, H. Minakata, and H. Nunokawa, Phys. Rev. **D72**, 033003 (2005), hep-ph/0504026.
- [63] S. K. Agarwalla, S. Prakash, S. K. Raut, and S. U. Sankar, JHEP **12**, 075 (2012), 1208.3644.
- [64] R. Acciarri et al. (DUNE) (2016), 1601.02984.
- [65] B. Choudhary, R. Gandhi, Sanjib. R. Mishra, Shekhar Mishra and J. Strait, *Proposal of Indian Institutions and Fermilab Collaboration for Participation in the Long-Baseline Neutrino Experiment at Fermilab*, "<http://lbne2-docdb.fnal.gov/cgi-bin/RetrieveFile?docid=6704&filename=LBNE-India-DPR-V12-Science.pdf&version=1>" (2012).
- [66] S. Choubey and D. Pramanik (2016), 1604.04731.
- [67] M. Masud and P. Mehta (2016), 1603.01380.
- [68] M. Masud and P. Mehta (2016), 1606.05662.
- [69] Elizabeth Worcester, private communication (2016).
- [70] M. Masud, A. Chatterjee, and P. Mehta (2015), 1510.08261.
- [71] P. Coloma, JHEP **03**, 016 (2016), 1511.06357.
- [72] A. de Gouvea and K. J. Kelly, Nucl. Phys. **B908**, 318 (2016), 1511.05562.
- [73] D. V. Forero and P. Huber (2016), 1601.03736.
- [74] J. Liao, D. Marfatia, and K. Whisnant, Phys. Rev. **D93**, 093016 (2016), 1601.00927.
- [75] K. Huitu, T. J. Karkkainen, J. Maalampi, and S. Vihonen, Phys. Rev. **D93**, 053016 (2016), 1601.07730.
- [76] P. Bakhti and Y. Farzan (2016), 1602.07099.

- [77] A. Rashed and A. Datta (2016), 1603.09031.
- [78] P. Coloma and T. Schwetz (2016), 1604.05772.
- [79] A. de Gouvea and K. J. Kelly (2016), 1605.09376.
- [80] M. Blennow, S. Choubey, T. Ohlsson, D. Pramanik, and S. K. Raut (2016), 1606.08851.